ORIGINAL PAPER

Experimental and theoretical study of dilute polyacrylamide solutions: effect of salt concentration

**Panke Chen · Lin Yao · Yanyan Liu · Jianhui Luo ·
Ge Zhou · Bo Jiang**

Abstract The structure and intrinsic viscosity of the partially hydrolyzed polyacrylamide (HAPM) and polyacrylamide (PAM) in aqueous solution were investigated by comparative studies of molecular dynamics simulation over a wide range of the NaCl concentration. The radius of gyration (R_g), the hydrodynamic radius (R_h) and the ratio of the radius gyration and the hydrodynamic radius (ρ) were calculated for the PAM or HPAM in solutions with different NaCl concentrations at 298 K. The conformational changes of the polymer chain in different aqueous solution were discussed according to the molecular shapes. It was found that the change of the R_h or the R_g can reflect the change in the $[\eta]$. And the changes in the structure of the polymer chain with different NaCl concentrations were discussed via the ρ which can predict $[\eta]$ changes. The results showed that behavior of the polymer solution calculated from the simulation agreed with the experimental measurements. Furthermore, the radial distribution functions for the HPAM solutions were investigated, which verified the micro-mechanism for the change of the structure. The results of
this research showed that the computational method used in this work has practical applicability.

Introduction

Polyacrylamide is a water-soluble, linear polymer. This polymer and its derivatives are applied in many industries such as agricultural, water treatment, medical, and petroleum industry [1, 2]. Especially in petroleum industry, non-ionic polyacrylamide (PAM) and partially hydrolyzed polyacrylamide (HPAM) are used for enhancing oil recovery. However, some factors, such as the rising temperature of the earth, the presence of salts in the drilling fluid medium, and the mechanical degradation of the polymer, decrease the viscosity of hydrolyzed PAM in the aqueous solution significantly, which limits the application of PAM. Some have focused on the investigation of the macroscopic properties of dilute solutions looking at the effect of temperature, pH, salt concentration and surfactant on the conformation of the polyacrylamide molecules [3–7]. Others have dealt with the microscopic properties and structures of dilute solutions explaining the macroscopic phenomena of the polymer [8–11].

However, using the experimental methods, it is still difficult to go into the microscopic mechanism for the changes of the structure and dimension of the polymer. Computer simulation technique [12, 13] can make up for the lack of experimental methods. The technique allows investigators to get a deeper understanding of properties versus different

P. Chen · L. Yao · Y. Liu · G. Zhou (✉) · B. Jiang
Key Laboratory of Green Chemistry and Technology,
Ministry of Education, College of Chemistry, Sichuan University,
Chengdu 610064, China
e-mail: zhougekk@scu.edu.cn

B. Jiang
e-mail: jiangbo@scu.edu.cn

J. Luo
Research Institute of Petroleum Exploration
and Development of PetroChina,
Beijing 100083, China

polymer structure and modify the polymer structure at molecular level [14, 15]. Many works are devoted to study the properties of polymer materials using the computer simulation which plays an ever-increasing role in predicting and designing polymer properties, and guiding such experimental work as synthesis and characterization.

In this work, the effect of NaCl concentration on the structures of the PAM and HPAM by computational and experimental methods is studied. In the computational section, some physical parameters were calculated at different models, such as the radius of gyration (R_g), the hydrodynamic radius (R_h), the intrinsic viscosity ([η]) and the radial distribution function (RDF). In experimental section, the intrinsic viscosities of the PAM and HPAM solutions as the varieties of NaCl concentration are investigated. And the relationships among [η], R_g and R_h are analyzed according to the references reported. Combining the two sections, we can make it the relationship between the microstructures and the macrostructures of PAM and HPAM.

Computational methodologies

All the dilute PAM and HPAM solution models were built using Materials Studio program (MS, version 4.2 Accelrys Software Inc., United States). Details of the construction and MD methods of the PAM and HPAM solution models are described below.

A PAM chain was composed of 50 repeat units acrylamide (AM) monomers, of which 25% of monomers were replaced randomly by sodium acrylate (NaAA) monomers to turn into a random HPAM chain (degree of hydrolysis, 25%). Their monomers were randomly connected to form the atactic conformations. The solution model is constructed by Amorphous Cell module. The molecule chains and ions were embedded into the cubic cells full of 2000 minimized water molecules with approximate 1 gcm^{-3} density to form the polymer solution models with a series of different NaCl concentrations. It is named according to the monomer, for example, the PAM means that it contains one polymer chain with acrylamide (AM) monomers and 2000 H$_2$O (with different NaCl concentrations). Part of the models have been shown in Fig. 1. In the dilute solution polymer chains are isolated from each other in the solvent [14]. The number of the ions was listed in Table 1 for various solution models. During this process, the Period Boundary Condition (PBC) [14] was taken and a cutoff radius of 10 Å was applied for both non-bonded electrostatic and van der Waals interactions.

Next, each initial model was optimized for the proper polymer conformations and distributions of solvent cluster by the Smart Minimizer method with no less than 10,000 iterations. And then, the NPT (constants number of
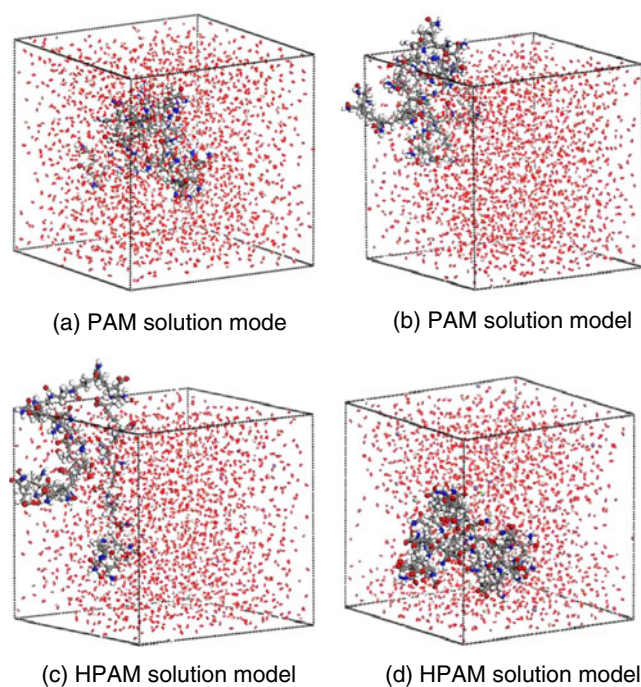

(a) PAM solution mode   (b) PAM solution model

(c) HPAM solution model   (d) HPAM solution model

Fig. 1 PAM or HPAM solution models without (a or c) and with 2% NaCl (b or d) at 298 K. Red ball: oxygen atom; Blue ball: nitrogen atom; White ball: hydrogen atom; Purple ball: sodium atom; Light green ball: chlorine atom

particles, press, and temperature, $P=1.01\times10^{-5}$ Mpa, $T=$ 298 K) ensemble conditions of MD simulation was assigned. To eliminate the gaps between molecules and gain the stable models closer to the real system, the models were annealed for first 120 ps (1 ns=10^3 ps=10^6 fs=10^{-9} s) changing temperature from 298 K to 418 K then 298 K at rate 2 K·ps^{-1}, and then 80 ps at 298 K. Finally, the MD stage of 3 ns MD (NVT ensemble, 298 K) followed. This was because the NVT [12] (constant number of particles, volume, and temperature $T=$298 K) could improve the computational efficiency compared with the NPT for the condensed phases. And separately computed 5 ns trajectories at 298 K proved to yield very similar results; therefore, 3 ns trajectories were used. The first 2 ns of each trajectory were used for equilibration, and the rest was used for data analysis. The time step in the MD simulations was 1 fs. The coordinates and energies of all molecules were saved every 1 ps for further analyses. The temperature and pressure were kept constant using the Andersen thermostat [16] and Berendsen barostat [17], respectively. In all simulations, the intra- and intermolecular interactions within the systems were determined by the polymer consistent force field (PCFF). PCFF is developed based on CFF91 and is intended for application to polymers. Consequently, this forcefield enables accurate and simultaneous prediction of structural, conformational, vibrational, and thermophysical properties for a broad range of molecules in isolation and in condensed

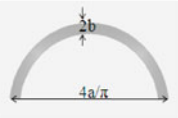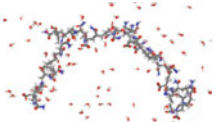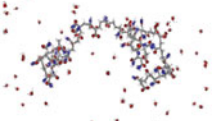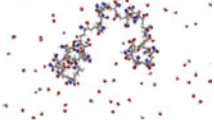**Table 1** Parameters for HPAM or PAM solution models at 298 K
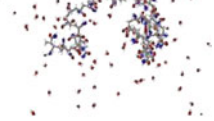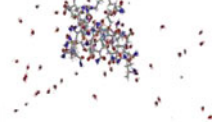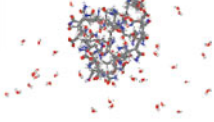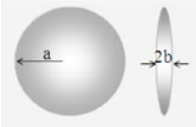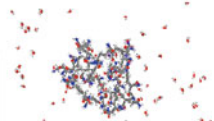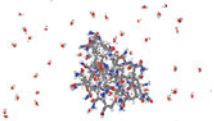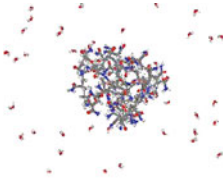
Solution model	Molecule shape	Snapshot of mean conformation from simulations	$w_{(NaCl)}$	N_{NaCl}	V_{cell} (nm^3)	$\rho_{NaCl} \times 10^3$ (g·cm^{-3})	ρ_{H2O} (g·cm^{-3})	ρ_P (g·cm^{-3})	$2a$ (nm)	λ
			0.0%	0	59.8	0	1	0.10	3.80	9.54
			0.1%	1	59.8	1.6	1	0.10	3.39	8.33
	Bent spheroid		0.3%	2	59.8	3.3	1	0.10	3.12	6.70
HPAM			0.7%	5	59.8	8.1	1	0.10	2.84	3.71
			1.0%	7	59.8	11.4	1	0.10	1.82	0.27
	Disk (spheroidal)		1.5%	10	59.8	16.3	1	0.10	1.85	0.33
			2.0%	14	59.8	22.8	1	0.10	1.80	0.33
PAM			0.0%	0	59.8	0	1	0.11	1.80	0.33
	Disk (spheroidal)		0.1%	1	59.8	1.6	1	0.11	1.80	0.33

Table 1 (continued)

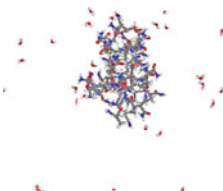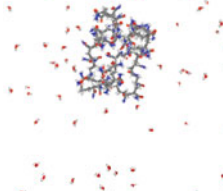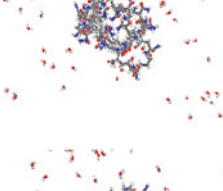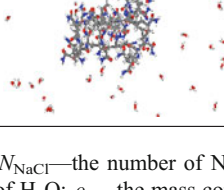| Solution model	Molecule shape	Snapshot of mean conformation from simulations	$w_{(NaCl)}$	N_{NaCl}	V_{cell} (nm^3)	$\rho_{NaCl} \times 10^3$ (g·cm^{-3})	ρ_{H2O} (g·cm^{-3})	ρ_P (g·cm^{-3})	$2a$ (nm)	λ
			0.3%	2	59.8	3.3	1	0.11	1.80	0.33
			0.7%	5	59.8	8.1	1	0.11	1.80	0.33
			1.1%	8	59.8	12.8	1	0.11	1.80	0.33
			1.5%	10	59.8	16.3	1	0.11	1.80	0.33
			2.0%	14	59.8	22.8	1	0.11	1.85	0.33

$w_{(NaCl)}$—the mass fraction for NaCl; N_{NaCl}—the number of NaCl molecule; V_{cell}—the volume for cubic cell; ρ_{NaCl}—the mass concentration of NaCl; ρ_{H2O}—the mass concentration of H$_2$O; ρ_P—the mass concentration of PAM or HPAM

phases, and under a wide range of conditions of temperature and pressure.

Experimental section

Materials

The PAM and HPAM (degree of hydrolysis, 25%) were provided by Research Institute of Petroleum Exploration and Development of PetroChina in Beijing of China with the weight average molecular weights ($\overline{M}_W$) of 2.6×10^6 and 1.5×10^6 g·mol^{-1}, respectively. And sodium chloride (NaCl) was analytically a pure grade agent. Water was distilled and deionized as solvent.

Methods

The PAM and HPAM original aqueous solutions and the solvents were prepared with different concentrations of NaCl ($w = 0 \sim 2\%$). The mass concentrations of the PAM

and HPAM original solutions were 0.01 g·cm^{-3} and 2.3×10^{-3} g·cm^{-3}, respectively. Viscometric measurements of the polymer solutions were carried out with a 0.57 mm Ubbelohde capillary viscometer at 25 ± 0.1 °C. And the intrinsic viscosity $[\eta]$ was determined by the single-concentration method using the Solomon and Ciuta equation [18]:

$$[\eta] = [2((\eta_r - 1) - \ln \eta_r)]^{1/2}/C, \tag{1}$$

where η_r is the relative viscosity obtained from the ratio of the flow times of a solution and the solvent and c is the polymer concentration. At least five flow times were recorded for each solution and the relative error in the flow times was less than 0.1%. Every experiment for the polymer solution was completed within 3 days.

Results and discussion

Size and shape

In this work, several interesting properties of PAM and HPAM solution models are studied as follows, which can mirror the effect of the solvents on the structures of PAM and HPAM.

The radius of gyration R_g (s) represents the molecular size of the polymer explored in this work, which is defined as the root mean square distance of the atoms in the molecule from their common center of mass, that is:

$$s^2 = \left(\sum_{i=1}^{N} m_i s_i^2 \right) / \left(\sum_{i=1}^{N} m_i \right), \tag{2}$$

where s_i denotes the distance of atom i from the center of mass and N denote the total number of atoms.

From all simulations, the mean conformation of every polymer in solution models can be gained as Table 1 shows. Adamczyk et al. has researched that the molecule shape for every polymer can be determined by the mean conformation and the hydrodynamic radius (R_h), the intrinsic viscosity $([\eta])$ for a polymer can be calculated by the parameters of the molecule shape (a and λ) and the equations [19, 20].

And the intrinsic viscosity $([\eta])$ for a polymer can be calculated by the parameters of the molecule shape (a and λ) and the equations in Ref. [19, 20]. For example, for bent spheroid,

$$\lambda = a/b > 1$$
$$R_h = 2a/2\left(\tfrac{11}{12}\ln\lambda - 0.31\right)$$
$$[\eta] = \lambda^2 \langle 3/[\ln(2\lambda) - 0.5] + 1/[\ln(2\lambda) - 1.5]\rangle/15 + 8/5 \tag{3}$$

and for the spheroidal disk,

$$\lambda = b/a < 1$$
$$R_h = a/(\lambda^2 \beta)$$
$$[\eta] = 5Q_1 - Q_2 + 2Q_3$$
$$\beta = \cos^{-1}\lambda / \left[\lambda(1 - \lambda^2)^{1/2}\right]$$
$$\alpha_\parallel = 2(\lambda^2\beta - 1)/(\lambda^2 - 1)$$
$$\alpha_\perp = \lambda^2(1 - \beta)/(\lambda^2 - 1)$$
$$\alpha_\parallel' = \lambda^2(3\beta + 2\lambda^2 - 5)/\left[4(\lambda^2 - 1)^2\right]$$
$$\alpha_\parallel'' = \lambda^2[2\lambda^2 + 1 - (4\lambda^2 - 1)\beta]/4(\lambda^2 - 1)^2$$
$$\alpha_\perp' = \lambda(\lambda^2 - 3\lambda^2\beta + 2)/(\lambda^2 - 1)$$
$$\alpha_\perp'' = \lambda^2[(2\lambda^2 + 1)/\beta - 3]/(\lambda^2 - 1)^2$$
$$Q_1 = 1/\left(5\alpha_\parallel'\right)$$
$$Q_2 = 2/\left[15\alpha_\parallel'\left(1 - \alpha_\parallel''/\alpha_\perp''\right)\right]$$
$$Q_3 = \left\langle \lambda(\alpha_\parallel + \alpha_\perp)\alpha_\parallel'/[(\lambda^2\alpha_\parallel + \alpha_\perp)\alpha_\perp'] - 1 \right\rangle/\left(5\alpha_\parallel''\right)$$

$$\tag{4}$$

So for our solution models, the hydrodynamic radius for the PAM or HPAM molecule and the intrinsic viscosity can be calculated by Eqs. (3) and (4) and the parameters of the molecule shape in Table 1.

In dilute solution, the intrinsic viscosity has been used to study the hydrodynamic volume of polymer chains and the interaction between polymer chains and solvent or between different polymer chains [21]. Previous researchers have reported reasonable results when they used less monomer for polymer simulation [22, 23]. As reported the intrinsic viscosity greatly depended on the salt concentration [6, 24]. When the HPAM is dissolved in deionized water, the HPAM macromolecule with the carboxylate groups (–COO$^-$) can form an electrical double layer and thick hydration film, which can pack more H$_2$O molecules. Thus the HPAM will extend and have larger hydrodynamic volume, accordingly the viscosity of solution will be higher. The NaCl added to the HPAM solution can ionize Na$^+$, which can destroy the electrostatic repulsion between the –COO$^-$ groups of the HPAM molecule chain and compress the electrical double layer around the –COO$^-$ groups and make the hydration film thinning [6, 25]. This leads the HPAM chain to a more collapsed conformation and smaller overall dimension. The viscosity of the system decreases. The higher the NaCl concentration is, the smaller the viscosity is [6, 24, 25]. As shown in Fig. 2, the intrinsic viscosity for HPAM solution decreases gradually with increasing NaCl concentration. However, the intrinsic viscosity of PAM solution has no evident change with increasing NaCl concentration. Due to the absence of ionic groups in the PAM chain, the PAM
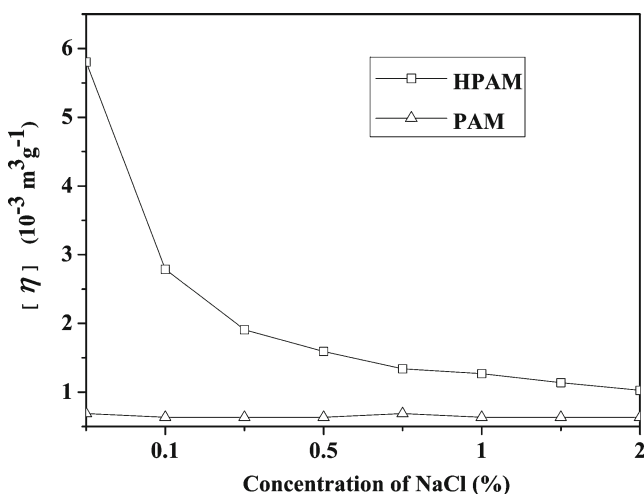
Fig. 2 The influence of NaCl concentration on the intrinsic viscosities of the original HPAM and PAM aqueous solution measured by experiments at 298 K

chain collapses under different NaCl concentration. The intrinsic viscosity value is smaller than the value for HPAM.

In addition, an approximation of the hydrodynamic radius (R_h) and the radius of gyration (R_g) of a polymeric molecule in a solvent is predict via [6, 26]

$$[\eta] = 10\pi R_h^3 dN_A / 3M_w \qquad (5)$$

$$[\eta] = 6^{3/2}\Phi R_g^3 / M_w \qquad (6)$$

with d the specific gravity of the solute, N_A the Avogadro number, M_w the molecular weight, and Φ the value reflecting the solvent quality [26]. According to Eq. (5), it is clear that the intrinsic viscosity is affected only by R_h and proportional to R_h^3. In Eq. (6), the intrinsic viscosity is determined by R_g^3 and Φ.

A dimensionless quantity ρ is defined as R_g/R_h which no longer depends on the bond length and the degree of polymerization but is a function of the branching density, of polydispersity, and of the inherent flexibility of the subchains [27]. Thus, ρ is sensitive to structural changes of polymer and increases as the structure or conformation extends. The ρ value can be estimated by combining Eq. (5) and (6)

$$\rho = R_g/R_h = \left[10\pi dN_A \Big/ \left(3 \times 6^{3/2}\right)\right]^{1/3} \Big/ \Phi^{1/3} \qquad (7)$$

ρ is inversely proportional to $\Phi^{1/3}$ which describes not only the conformation change of the polymer molecule but also the solvation power of HPAM or PAM in different solutions.

Using MD simulations, the change trends of R_h for HPAM or PAM were investigated which reflects the trend of intrinsic viscosity in the polymer solutions with different

concentrations of NaCl. Simultaneously, R_g for HPAM or PAM can be gained using MD simulations to explore solvation power of the polymer under different NaCl concentrations. In Figs. 3 and 4 the R_g, R_h and $[\eta]$ for HPAM or PAM vs concentration of NaCl are shown. The viscosity of HPAM decreases and PAM solution has no apparent change with increasing NaCl concentration. $[\eta]$ changes with increasing NaCl concentrations are in good agreement with the experimental results (Fig. 2). Furthermore, it is found that the trends of R_g, R_h and $[\eta]$ are similar in Figs. 3 and 4. It implies that R_g^3 compared with Φ plays a more important role in Eq. (6) for our solution systems. Consequently, Φ is used as a constant in Eq. (6) [19]. The R_h, R_g can be used to predict $[\eta]$ changes for HPAM or PAM solutions with different concentrations of NaCl as Eqs. (5 and 6) show.

The values of ρ (R_g/R_h) for the HPAM solution models are represented in Fig. 3(c) as a function of NaCl concentration and for the PAM solution models in Fig. 4(c). In Fig. 3(c) a minor decrease becomes noticeable, and in Fig. 4 (c) almost no change occurs. The trend of ρ and $[\eta]$ are similar to each other. It indicates ρ also could predict $[\eta]$ changes. For the HPAM the decrease of ρ from 1.58 to 1.20 displays the transition from an extended coil to a collapsed coil (Table 1) with increasing solvation power. However for the PAM there is no significant change of ρ in 1.10, it implies the structure to be a collapsed coil (Table 1) and the solvation power are not affected basically as NaCl

Fig. 3 The influence of NaCl concentration on the parameters [Radius of gyration (**a**), hydrodynamic radius (**b**), the ratio of the radius of gyration and the hydrodynamic radius (**c**) and intrinsic viscosity (**d**)] of HPAM solution models at 298 K
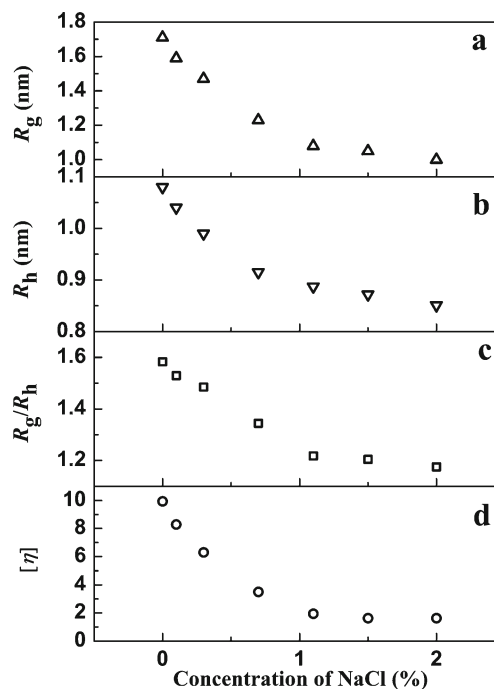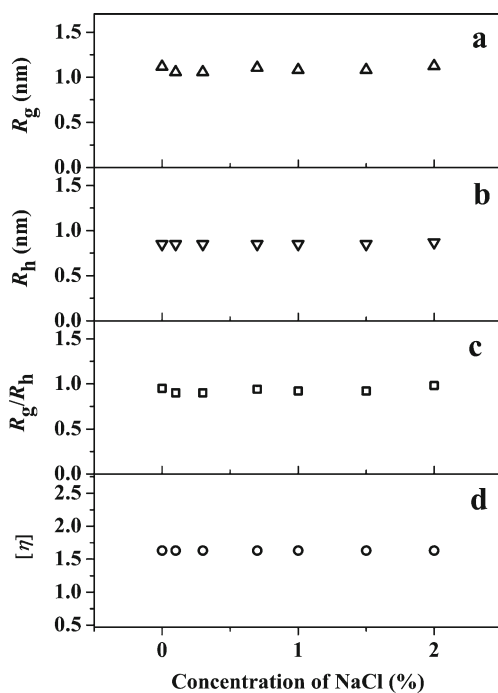
Fig. 4 The influence of NaCl concentration on the parameters [Radius of gyration (**a**), hydrodynamic radius (**b**), the ratio of the radius of gyration and the hydrodynamic radius (**c**) and intrinsic viscosity (**d**)] of PAM solution models at 298 K

concentration increases. The simulation trend is in agreement with the experimental research [6, 24, 25]. The HPAM chain changes from an extended coil to collapsed coil with the addition of NaCl. So the R_g, R_h and $[\eta]$ for the HPAM reduce in the aqueous solutions as the varieties of NaCl concentrations. While for the R_g, R_h and $[\eta]$ for PAM no evident change is shown with the addition of NaCl.

The radial distribution function

The radial distribution function $g(r)$ can be calculated for either one or two sets of atoms via

$$g(r) = \left[\sum_{i=1}^{N} \sum_{j \neq 1}^{N} \delta(r - r_{ij}) \right] / N, \tag{8}$$

where r_{ij} is the distance between a pair of atoms or centroids.

Many investigators have considered that the electrostatic repulsion for the –COO⁻ groups hydrated lead to extend the polymer chain, and the addition of NaCl made the hydration film thinner, thus the electrostatic repulsion was screened, the polymer chain becomes more flexible, leading the polymer chain to a more collapsed conformation and to smaller overall dimension [6, 24, 25]. However, no one has accounted for the effect of NaCl on the hydration of the –COO⁻ groups of the HPAM from microscopic view. It is
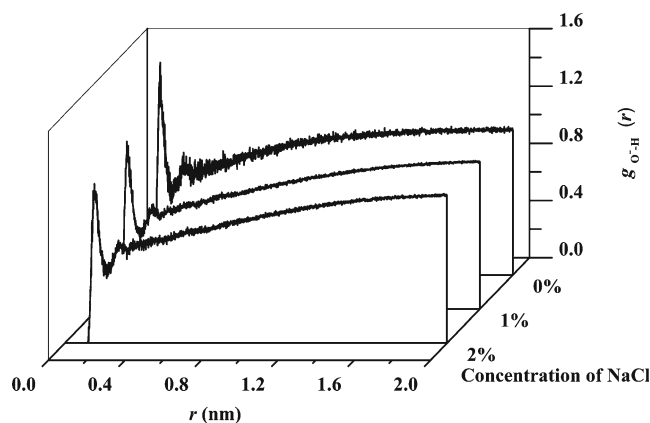

Fig. 5 RDF for O⁻ (–COO⁻) of HPAM and H (H₂O) with different concentrations of NaCl at 298 K

reported that the radial distribution function can be used to study the interaction between atoms, molecules or an atom and a molecule, including hydration [28].

Figures 5 and 6 show the O⁻ of the –COO⁻ group of the HPAM and H_2O radial distribution function $g_{O^--H}(r)$ and the O of the –CONH₂ group of the HPAM and H_2O radial distribution function $g_{O-H}(r)$ at different NaCl concentrations ($w=0\%$、1%、2%). It is clear that at 0.16 nm the first peak of $g_{O^--H}(r)$ is 1.46, 1.37 and 1.09 respectively with increasing NaCl concentration indicating decreasing interaction between O⁻ and H_2O. This verifies that the NaCl in aqueous solution destroyed the hydration layer of the O⁻ in the HPAM by weakening the electrostatic repulsion between the –COO⁻ groups of the HPAM so that the HPAM chain transforms from an extended coil to a collapsed coil and the dimension of the HPAM decreases as the NaCl concentration increases. Compared with $g_{O^--H}(r)$, the first peak of $g_{O-H}(r)$ arises at 0.18 nm, it implies a longer distance between O and H_2O. The first peak has no significant change with increasing NaCl concentration. It implies the hydration of the O of the PAM is very weak and not influenced basically by increasing NaCl concentration.
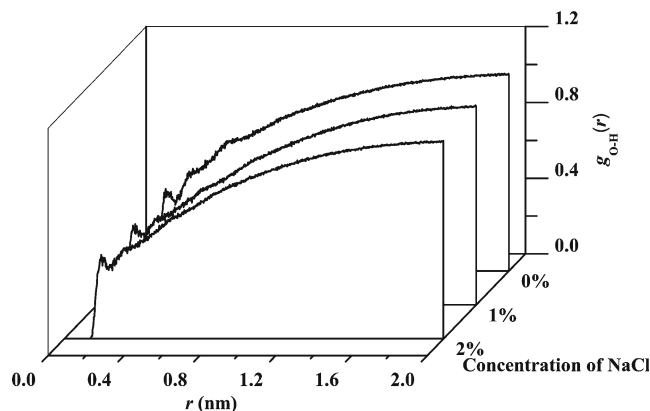

Fig. 6 RDF for O (–CONH₂) of PAM and H (H₂O) with different concentrations of NaCl at 298 K

Conclusions

The structure and intrinsic viscosity of the HAPM and PAM in aqueous solution were calculated by molecular dynamics simulation method and compared to experimental values of viscosity over a wide range of the NaCl concentration. The simulation results showed that the hydrodynamic radius, the radius of gyration and the intrinsic viscosity for the HPAM chain decrease with the increasing NaCl concentration and exhibits no significant change for PAM solution. The molecular dynamic method can be effectively used to monitor the viscosity dependence of the polymer solution on NaCl concentration. The dimensionless quantity ρ defined as R_g/R_h describes well the conformational properties of the HAPM and PAM chain in aqueous solution as well as their viscosity behaviors. The radial distribution functions $g(r)$ at different NaCl concentrations give a good explanation about the conformational changes of the HAPM or PAM in NaCl solution on the molecular level. The molecular dynamics simulation is an effective tool for the conformational and viscosity properties of the polymer solution, which can provide useful information for the synthesis of polyacrylamide derivatives with desired solution properties.

References

1. Schuberth S, Münstedt H (2008) Transient elongational viscosities of aqueous polyacrylamide solutions measured with an optical rheometer. Rheol Acta 47:139–147
2. Xu LN (2008) Viscoelasticity of mixed polyacrylamide solution. J Cent South Univ Technol 15:443–446
3. Gouveia LM, Müller AJ, Marchal P, Choplin L (2008) Time effects on the rheological behavior of hydrophobically modified polyacrylamide aqueous solutions mixed with sodium dodecyl sulfate (SDS). Colloids Surf A Physicochem Eng Aspects 330:168–175
4. Yahaya GO, Ahdab AA, Ali SA, Abu-Sharkh BF, Hamad EZ (2001) Solution behavior of hydrophobically associating water-soluble block copolymers of acrylamide and N-benzylacrylamide. Polymer 42:3363–3372
5. Ma JT, Liang B, Cui P, Dai H, Huang RH (2003) Dilute solution properties of hydrophobically associating polyacrylamide: fitted by different equations. Polymer 44:1281–1286
6. Gong HJ, Xin X, Xu GY, Wang YJ (2008) The dynamic interfacial tension between HPAN/C17H33COONa mixed solution and crude oil in the presence of sodium halide. Colloids Surf A Physicochem Eng Aspects 317:522–527
7. Gouveia LM, Müller AJ (2009) The effect of NaCl addition on the rheological behavior of cetyltrimethylammonium p-toluenesulfonate (CTAT) aqueous solutions and their mixtures with hydrophobically modified polyacrylamide aqueous solutions. Rheol Acta 48:163–175
8. Zhang YB, Wu C, Fang Q, Zhang YX (1996) A light-scattering study of the aggregation behavior of fluorocabon-modified polyacrylamides in water. Macromolecules 29:2494–2497
9. Klucker R, Munch JP, Schosseler F (1997) Combined static and dynamic light scattering study of associating random block copolymers in solution. Macromolecules 30:3839–3848
10. Buhler E, Rinaudo M (2000) Structural and dynamical properties of semirigid polyelectrolyte solutions: A light-scattering study. Macromol 33:2098–2106
11. Ravichandran S, Ramanathan K (2008) Molecular interactions with polyacrylamide in ethanolamine, diethanolamine, and triethanolamine solutions measured ultrasonically. Polym Plast Technol En 47:169–173
12. Ungerer P, Nieto-Draghi C, Rousseau B, Ahunbay G, Lachet V (2007) Molecylar simulation of the thermophysical properties of fluids: from understanding toward quantitative predictions. J Mol Liq 134:71–89
13. Rangou S, Theodorakis PE, Gergidis LN, Avgeropoulos A, Efthymiopoulos P, Smyrnaios D, Kosmas M, Vlahos C, Giannopoulos T (2007) Synthesis, molecular characterization and theoretical study of first generation dendritic homopolymers of butadiene and isoprene with different microstructures. Polymer 48:652–663
14. Fu CL, Ou-Yang WZ, Sun ZY, An LJ, Li HF, Tong Z (2009) Solvent size effect on the static and dynamic properties of polymer chains in athermal solvents. Polymer 50:5142–5148
15. Dalakoglou GK, Karatasos K, Lyulin SV, Lyulin AV (2007) Brownian dynamics simulations of complexes of hyperbranched polymers with linear polyelectrolytes: effects of the strength of electrostatic interaction on static properties. J Chem Phys 127:214903
16. Andersen HC (1980) Molecular dynamics simulations at constant pressure and/or temperature. J Chem Phys 72:2384–2393
17. Berendsen HJC, Postma JPM, van Gunsteren WF, DiNola A, Haak JR (1984) Molecular dynamics with coupling to an external bath. J Chem Phys 81:3684–3690
18. Hong LZ, Liu GJ (2010) Viscometric study of poly(2-cinnamoyloxyethyl methacrylate). Macromolecules 43:3941–3946
19. Adamczyk Z, Jachimska B, Jasiński T, Warszyński P, Wasilewska M (2009) Structure of poly(sodium 4-styrenesulfonate) (PSS) in electrolyte solutions: theoretical modeling and measurements. Colloids Surf A Physicochem Eng Aspects 343:96–103
20. Adamczyk Z, Bratek A, Jachimska B, Jasiński T, Warszyński P (2006) Structure of poly(acrylic acid) in electrolyte solutions determined from simulations and viscosity measurements. J Phys Chem B 110:22426–22435
21. Cho J, Heuzey MC, Bégin A, Carreau PJ (2006) Viscoelastic properties of chitosan solutions: effect of concentration and ionic strength. J Food Eng 74:500–515
22. Bishop M, Kalos MH, Frisch HL (1979) Molecular dynamics of polymeric systems. J Chem Phys 70:1299–1304
23. Pan R, Liu XK, Zhang AM, Gu Y (2007) Molecular simulation on structure-property relationship of polyimides with methylene spacing groups in biphenyl side chain. Comput Mater Sci 39:887–895
24. Ikeda Y, Beer M, Schmidt M, Huber K (1998) Ca^{2+} and Cu^{2+} induced conformational changes of sodium polymethacrylate in dilute aqueous solution. Macromolecules 31:728–733
25. Zhou H, Song GQ, Zhang YX, Chen JY, Jiang M, Hogen-Esch TE, Dieing R, Ma L, Haeussling L (2001) Hydrophobically modified polyelectrolytes, 4 Synthesis and solution properties of fluorocarbon-containing poly(acrylic acid). Macromol Chem Phys 202:3057–3064
26. Kairn T, Daivis PJ, Matin ML, Snook IK (2004) Concentration dependence of viscometric properties of model short chain polymer solutions. Polymer 45:2453–2464
27. Burchard W, Schmidt M, Stockmayert WH (1980) Information on polydispersity and branching from combined quasi-elastic and intergrated scattering. Macromolecules 13:1265–1272
28. Gnanasambandam S, Hu ZQ, Jiang JW, Rajagopalan R (2009) Force field for molecular dynamics studies of glycine/water mixtures in crystal/solution environments. J Phys Chem B 113:752–758